

Joint Resource-Power Allocation and UE Rank Selection in Multi-User MIMO Systems with Linear Transceivers

K. Pavan Srinath, *Member, IEEE*, Alix Jeannerot, and Alvaro Valcarce Rial, *Senior Member, IEEE*

Abstract—Next-generation wireless networks aim to deliver data speeds much faster than 5G. This requires base stations with lots of antennas and a large operating bandwidth. These advanced base stations are expected to serve several multi-antenna user-equipment (UEs) simultaneously on the same time-frequency resources on both the uplink and the downlink. The UE data rates are affected by the following three main factors: *UE rank*, which refers to the number of data layers used by each UE, *UE frequency allocation*, which refers to the assignment of slices of the overall frequency band to use for each UE in an orthogonal frequency-division multiplexing (OFDM) system, and *UE power allocation/control*, which refers to the allocation of power by the base station for data transmission to each UE on the downlink or the power used by each UE to send data on the uplink. Since multiple UEs are to be simultaneously served, the type of precoder used for downlink transmission and the type of receiver used for uplink reception predominantly influence these three aforementioned factors and the resulting overall UE throughput. This paper addresses the problem of jointly selecting these three parameters specifically when zero-forcing (ZF) precoders are used for downlink transmission and linear minimum mean square error (LMMSE) receivers are employed for uplink reception.

Index Terms—Joint resource-power allocation, linear minimum mean square error (LMMSE) receiver, multi-user MIMO (MU-MIMO), OFDM, UE rank selection, ZF precoders.

I. INTRODUCTION

Next generation wireless systems, often referred to as 6G, are being actively researched to address the ever-growing demand for data and connectivity. These systems aim to go beyond the capabilities of 5G New Radio (5G NR), offering significantly faster speeds, ultra-low latency, and the ability to connect a vast number of devices. 6G has the potential to revolutionize various fields, from enabling real-time remote surgery to supporting entirely new applications like Extended Reality (XR). It is expected that 6G base stations (BSs) will be equipped with a much larger number of transceiver chains in the range 128 – 512 compared to 32 – 64 in a typical 5G BS, and will operate over larger bandwidths in the range 200 – 400 MHz compared to 100 MHz in 5G. Each BS is expected to serve around 10 – 20 user-equipment (UEs) in the same time-frequency resource during peak traffic hours, and this is called *extreme multi-user multiple-input multiple-output (MU-MIMO)* transmission.

K. P. Srinath and A. Valcarce Rial are with Nokia Bell Labs, 91300 MASSY, France (email: {pavan.koteshwar_srinath, alvaro.valcarce_rial}@nokia-bell-labs.com), and A. Jeannerot is at INSA Lyon, Inria, CITI, UR3720, 69621 Villeurbanne, France (email: alix.jeannerot@inria.fr). A significant part of this work was done when A. Jeannerot was at Nokia Bell Labs, 91300 MASSY, France.

To maximize the resource utilization efficiency and the UE data rates, the following three procedures are essential: *UE rank selection*, which refers to deciding on the number of data layers that a UE uses for data transmission, *UE resource allocation*, where the system identifies which slices of the overall frequency band get assigned to a particular UE in an orthogonal frequency-division multiplexing (OFDM) system, and *UE power allocation/control*, which determines how much power a UE uses to send data (uplink) and how much power the BS allocates to send data to the user (downlink).

In single-user MIMO (SU-MIMO) transmissions, the orthogonal frequency-division multiple access (OFDMA) scheme avoids inter-user interference within the same cell. However, when multiple UEs are co-scheduled for transmission in the same time-frequency resources in a time slot, their respective transmitted data signals from the BS (downlink) or their respective received data signals at the BS (uplink) could potentially interfere with one another. The exact degree of this interference depends on the spatial correlation between the channels of the paired UEs, the type of MU-MIMO precoder used at the BS (downlink), and the type of MU-MIMO detector used at the BS (uplink). Therefore, the resulting UE data rates depend on how the frequency resources are shared between the UEs and this in turn influences the respective UE ranks and power allocation. Much of the literature has focused on optimizing these three procedures separately, but this leads to numerous balloon-effects where optimizing one resource reduces the gains achievable by optimizing another. Furthermore, up until the recent advent of 5G NR, MU-MIMO was not commonly used which has also delayed the development of joint solutions for this problem. Practical solutions for the joint allocation of time-frequency resources, power control, and rank selection remain elusive and are much needed for 6G MU-MIMO to succeed.

This paper addresses the problem of joint resource-power allocation and rank selection for a class of linear transceivers. In particular, we consider zero-forcing (ZF) precoders [1] for downlink (DL) transmission and linear minimum mean square error (LMMSE) receivers for uplink (UL) reception. We show that both these problems can be formulated under a common framework. Since the problems involve mixed integer programming for which finding the optimal solution could be computationally intensive, we provide a practically-feasible approach to obtain a reasonably good (even if possibly sub-optimal) solution. To the best of our knowledge, this is the first such work on jointly selecting the three aforementioned

features based on the type of precoder or receiver used.

Related Literature: In 5G NR and previous generations, UE rank selection, transmit power allocation for the downlink and UE power control for the uplink, and frequency allocation are done independently from one another and in sequence. This means that each feature operates within the constraints imposed by the decision made by the previous step. For UE rank selection, the BS might use the rank indicator (RI) sent by the UE or select the rank through capacity optimization [2] for both the uplink and the downlink. This is effective for SU-MIMO but not for MU-MIMO.

For UE uplink power control, the goal is to obtain good UE rates while minimizing the effect of inter-cell interference (ICI) (which occurs due to the uplink transmissions from the UEs in the neighbouring cells) and maintaining spectral flatness across multi-UE receptions. The open loop power control (OLPC) parameters P_0 and α for a UE are configured either statically or dynamically [3]. The values of these parameters ultimately specify the UL transmit power for that UE. These are effective for SU-MIMO transmission but are not tailored to MU-MIMO transmission due to unaccounted intra-cell interference, i.e., the interference from the co-scheduled UEs in the same cell. For frequency allocation, most commercial schedulers use round-robin frequency-domain scheduling [4] but stop short of a joint scheduling and power control solution.

For the downlink, there is a rich literature on how to design precoders (along with power allocation) for MU-MIMO [5], but these assume that the UE ranks and their allocated physical resource blocks (PRBs) have been fixed. ZF precoders [1] are more commonly used than minimum mean square error (MMSE) precoders because they suppress inter-user interference and their design does not require multiple iterations. For downlink frequency allocation, [6], [7] discuss a few reinforcement learning-based techniques. However, [6] is limited to SU-MIMO transmission with the allocation of frequency resources being independent of UE rank and power allocation while [7] addresses joint UE rank and resource allocation for MU-MIMO transmission without power allocation.

Paper Organization: The system model and a few relevant definitions are presented in Section II. Section III introduces the joint resource-power allocation and UE rank selection problem while Section IV details the proposed method that provides a practical way to obtain a reasonably good solution to this problem. Simulation results showing the efficacy of the proposed technique compared to some baseline schemes are presented in Section V, and concluding remarks constitute Section VI.

Notation: Boldface upper-case (lower-case) letters denote matrices (vectors). The field of complex numbers and the field of real numbers are respectively denoted by \mathbb{C} and \mathbb{R} . For any set \mathcal{S} , $|\mathcal{S}|$ denotes its cardinality if it is finite and the notation $\mathbf{X} \in \mathcal{S}^{m \times n}$ denotes that \mathbf{X} is a matrix of size $m \times n$ with each entry taking values from \mathcal{S} . For a matrix \mathbf{X} , its transpose and Hermitian transpose are respectively denoted by \mathbf{X}^T and \mathbf{X}^H , Frobenius norm by $\|\mathbf{X}\|$, and its $(i, j)^{th}$ entry by $[\mathbf{X}]_{i,j}$. The block-diagonal matrix with diagonal blocks $\mathbf{D}_1, \mathbf{D}_2, \dots, \mathbf{D}_n$ is denoted by $\text{diag}[\mathbf{D}_1, \mathbf{D}_2, \dots, \mathbf{D}_n]$, and the same notation is used for denoting a diagonal matrix with

diagonal elements d_1, \dots, d_n . The identity matrix and the null matrix are respectively denoted by \mathbf{I} and \mathbf{O} with their sizes understood from context. Finally, $\mathbb{I}_{\{A\}}$ denotes the indicator function for event A ; $\mathbb{I}_{\{A\}} = 1$ if A occurs, and is 0 otherwise.

II. SYSTEM MODEL

We consider an OFDM-based multiple-input multiple-output (MIMO) communication system with n_F subcarriers. A resource element (RE) corresponds to a subcarrier-OFDM symbol pair in the OFDM grid. A *slot* consists of T OFDM symbols (usually $T = 12$ or 14) and a PRB consists of 12 subcarriers. Suppose that the BS is equipped with n_B antennas and serves a set of $N_{UE} \geq 1$ co-scheduled UEs, with UE i equipped with $n_U^{(i)}$ antennas, $i = 1, \dots, N_{UE}$. Each UE i is assigned a rank (also called the number of data layers or spatial streams assigned for that UE) $n_L^{(i)} \leq n_U^{(i)}$ with $n_L \triangleq \sum_{i=1}^{N_{UE}} n_L^{(i)} \leq n_B$. Let $\mathbf{H}_{i,f,t} \in \mathbb{C}^{n_B \times n_U^{(i)}}$ denote the channel matrix between UE i and the BS for RE (f, t) , where f corresponds to the subcarrier index and $t = 1, \dots, T$, to the OFDM symbol index. While it is assumed that the BS has perfect knowledge of this channel-state information (CSI), in practice, only imperfect estimates are available, either through sounding reference signal (SRS) [8, Sec. 6.4.1.4] transmission on the uplink in a time division duplex (TDD) system or through UE CSI feedback in a frequency division duplex (FDD) system. Moreover, these estimates are only available at a certain granularity (e.g., one channel estimate for every two consecutive PRBs). In this paper, we call this set of contiguous PRBs for which a single channel estimate is available a physical resource block group (PRBG). This can also be a group of PRBs over which the channel is approximately constant. Therefore, *resource allocation refers to the assignment of PRBGs to the N_{UE} UEs that are to be served in the slot in context in order to optimize a certain performance metric, with possibly multiple UEs sharing the same PRBG*. It is assumed that once a PRBG is assigned to a UE, all the T OFDM symbols are used for communication by the UE in that PRBG. The constellation used for communication between the BS and UE i is a unit energy QAM constellation of size 2^{m_i} for some $m_i = 2, 4, 6, 8, \dots$, and is denoted by \mathcal{Q}_i .

A. Uplink transmission

Let $\mathbf{W}_{i,f,t} \in \mathbb{C}^{n_U^{(i)} \times n_L^{(i)}}$ be the precoding matrix used by UE i , with each column of $\mathbf{W}_{i,f,t}$ having unit norm. Let $\mathcal{I}_{f,t} \subseteq \{1, \dots, N_{UE}\}$ denote the set of indices of the UEs that have been allocated the PRBG that (f, t) belongs to. Suppose that UE $i \in \mathcal{I}_{f,t}$ transmits $\mathbf{x}_{i,f,t} \triangleq [x_{1,i,f,t}, \dots, x_{n_L^{(i)},i,f,t}]^T \in \mathcal{Q}_i^{n_L^{(i)} \times 1}$ on RE (f, t) , with each entry of $\mathbf{x}_{i,f,t}$ taking values from \mathcal{Q}_i . Further, let $p_{i,j,f,t} > 0$ denote the transmit power used by UE i for the j^{th} layer on RE (f, t) with $p_{i,j,f,t} = 0, \forall j$, if $i \notin \mathcal{I}_{f,t}$, and $\mathbf{D}_{i,f,t} \triangleq \text{diag}[\sqrt{p_{i,1,f,t}}, \dots, \sqrt{p_{i,n_L^{(i)},f,t}}] \in \mathbb{R}^{n_L^{(i)} \times n_L^{(i)}}$. With a maximum UE transmit power of $P_{U,max}$, it follows that

$$\sum_{f=1}^{n_F} \sum_{j=1}^{n_L^{(i)}} p_{i,j,f,t} \leq P_{U,max}, \forall i, \forall t. \quad (1)$$

With $n_{L,f,t} \triangleq \sum_{i \in \mathcal{I}_{f,t}} n_l^{(i)}$ being the total number of layers on RE (f,t) , the signal model for RE (f,t) is

$$\mathbf{y}_{f,t} = \sum_{i \in \mathcal{I}_{f,t}} \mathbf{H}_{i,f,t} \mathbf{W}_{i,f,t} \mathbf{D}_{i,f,t} \mathbf{x}_{i,f,t} + \mathbf{n}_{f,t} = \bar{\mathbf{H}}_{f,t} \mathbf{x}_{f,t} + \mathbf{n}_{f,t} \quad (2)$$

where $\mathbf{y}_{f,t} \in \mathbb{C}^{n_B \times 1}$, $\bar{\mathbf{H}}_{f,t} \in \mathbb{C}^{n_B \times n_{L,f,t}}$ is the effective channel matrix obtained by stacking the matrices $\{\mathbf{H}_{i,f,t} \mathbf{W}_{i,f,t} \mathbf{D}_{i,f,t}, i \in \mathcal{I}_{f,t}\}$ column-wise, $\mathbf{x}_{f,t}$ is a vector of size $n_{L,f,t}$ obtained by stacking the elements of $\{\mathbf{x}_{i,f,t}, i \in \mathcal{I}_{f,t}\}$ one below the other, and $\mathbf{n}_{f,t} \in \mathbb{C}^{n_B \times 1}$ is interference-plus-noise (including ICI) with mean $\mathbf{0}$ and covariance matrix $\mathbf{R}_{f,t} \in \mathbb{C}^{n_B \times n_B}$. After noise-whitening, we have

$$\mathbf{y}'_{f,t} \triangleq \mathbf{R}_{f,t}^{-1/2} \mathbf{y}_{f,t} = \mathbf{H}'_{f,t} \mathbf{x}_{f,t} + \mathbf{n}'_{f,t} \quad (3)$$

where $\mathbf{H}'_{f,t} \triangleq \mathbf{R}_{f,t}^{-1/2} \bar{\mathbf{H}}_{f,t} \in \mathbb{C}^{n_B \times n_{L,f,t}}$, and $\mathbf{n}'_{f,t}$ has covariance \mathbf{I} and is approximated to be standard complex additive white Gaussian noise (AWGN). LMMSE detection [9, Ch. 8] involves equalization using the matrix $\mathbf{G}_{f,t} \triangleq \left[\left(\mathbf{H}'_{f,t} \right)^H \mathbf{H}'_{f,t} + \mathbf{I} \right]^{-1} \left(\mathbf{H}'_{f,t} \right)^H \in \mathbb{C}^{n_{L,f,t} \times n_B}$, resulting in

$$\mathbf{G}_{f,t} \mathbf{y}'_{f,t} = \mathbf{G}_{f,t} \mathbf{H}'_{f,t} \mathbf{x}_{f,t} + \mathbf{G}_{f,t} \mathbf{n}'_{f,t}. \quad (4)$$

Except for the very low signal-to-noise ratio (SNR) regime, the performance of an LMMSE detector is close to that of a ZF detector [9, Ch. 8] which uses $\mathbf{G}_{f,t} \triangleq \left[\left(\mathbf{H}'_{f,t} \right)^H \mathbf{H}'_{f,t} \right]^{-1} \left(\mathbf{H}'_{f,t} \right)^H \in \mathbb{C}^{n_{L,f,t} \times n_B}$. In this case, the post-equalization signal-to-interference-noise ratio (SINR) for the j^{th} received symbol of UE i , $i \in \mathcal{I}_{f,t}$, $j = 1, \dots, n_l^{(i)}$, on RE (f,t) , is given as

$$\rho_{i,j,f,t} = \frac{1}{\left[\left[\left(\mathbf{H}'_{f,t} \right)^H \mathbf{H}'_{f,t} \right]^{-1} \right]_{l,l}} \quad (5)$$

where l corresponds to the position of the j^{th} symbol in the vector $\mathbf{x}_{f,t}$. So, while the LMMSE detector is superior to a ZF detector, especially for ill-conditioned MIMO channels, (5) is still a good approximation and a simpler closed-form expression for the post-equalization SINR obtained using an LMMSE detector.

B. Downlink transmission

With $\mathcal{I}_{f,t}$ and $n_{L,f,t}$ as defined in the previous subsection, let $\mathbf{W}_{i,f,t} \in \mathbb{C}^{n_B \times n_l^{(i)}}$ denote the part of the precoding matrix associated with UE i if $i \in \mathcal{I}_{f,t}$. Then, the overall precoding matrix $\mathbf{W}_{f,t} \in \mathbb{C}^{n_B \times n_{L,f,t}}$ used by the BS is obtained by stacking the matrices $\{\mathbf{W}_{i,f,t}, i \in \mathcal{I}_{f,t}\}$ column-wise, with each column of $\mathbf{W}_{f,t}$ having unit norm. Further, let $a_{k,i,j,f,t} \triangleq |\left[\mathbf{W}_{i,f,t} \right]_{k,j}|^2$, $k = 1, \dots, n_B$, $j = 1, \dots, n_l^{(i)}$. The BS transmits $\mathbf{x}_{i,f,t} \triangleq \left[x_{i,1,f,t}, \dots, x_{i,n_l^{(i)},f,t} \right]^T \in \mathcal{Q}_i^{n_l^{(i)} \times 1}$ on RE (f,t) to UE i if $i \in \mathcal{I}_{f,t}$, and uses a transmit power $p_{i,j,f,t} > 0$ for the j^{th} layer of UE i ($p_{i,j,f,t} = 0$ if $i \notin \mathcal{I}_{f,t}$). Let $\mathbf{D}_{i,f,t} \triangleq \text{diag} \left[\sqrt{p_{i,1,f,t}}, \dots, \sqrt{p_{i,n_l^{(i)},f,t}} \right]$. With a maximum BS transmit power of $P_{B,max}$ and a per-antenna

power constraint (PAPC) of $P_{ant} = P_{B,max}/n_B$, it follows that $\forall t = 1, \dots, T$,

$$\sum_{k=1}^{n_B} \sum_{i \in \mathcal{I}_{f,t}} \sum_{j=1}^{n_l^{(i)}} \sum_{f=1}^{n_F} a_{k,i,j,f,t} p_{i,j,f,t} \leq P_{B,max}, \quad (6)$$

$$\sum_{i \in \mathcal{I}_{f,t}} \sum_{j=1}^{n_l^{(i)}} \sum_{f=1}^{n_F} a_{k,i,j,f,t} p_{i,j,f,t} \leq P_{ant}, \quad (7)$$

$\forall k = 1, \dots, n_B$ in (7). In this paper, we consider the class of precoders called ZF precoders [1] that satisfy, for any $j, i \in \mathcal{I}_{f,t}$, $\mathbf{H}_{j,f,t}^T \mathbf{W}_{i,f,t} = \mathbf{0}$ when $j \neq i$, and $\mathbf{H}_{i,f,t}^T \mathbf{W}_{i,f,t} = \mathbf{U}_{i,f,t} \mathbf{\Lambda}_{i,f,t}$ for some matrix $\mathbf{U}_{i,f,t} \in \mathbb{C}^{n_B^{(i)} \times n_l^{(i)}}$ satisfying $\mathbf{U}_{i,f,t}^H \mathbf{U}_{i,f,t} = \mathbf{I}$ and $\mathbf{\Lambda}_{i,f,t} = \text{diag} \left[\sqrt{\lambda_{i,1,f,t}}, \dots, \sqrt{\lambda_{i,n_l^{(i)},f,t}} \right]$ with positive real-valued diagonal elements. With this, the signal model for the received signal at UE i on RE (f,t) is

$$\mathbf{y}_{i,f,t} = \mathbf{H}_{i,f,t}^T \mathbf{W}_{i,f,t} \mathbf{D}_{i,f,t} \mathbf{x}_{i,f,t} + \mathbf{n}_{i,f,t} \quad (8)$$

where $\mathbf{n}_{i,f,t} \in \mathbb{C}^{n_B^{(i)} \times 1}$ is the interference-plus-noise with mean $\mathbf{0}$ and covariance matrix $\mathbf{R}_{i,f,t} \in \mathbb{C}^{n_B^{(i)} \times n_B^{(i)}}$. Unlike the BS receiver which has several receive antennas resulting in colored interference noise on the uplink, the UE has only a few antennas, typically ranging from 2 to 8. Hence, $\mathbf{R}_{i,f,t} \approx \sigma_i^2 \mathbf{I}$ for some positive real-valued σ_i . After receiver equalization, we have

$$\mathbf{y}'_{i,f,t} \triangleq \mathbf{U}_{i,f,t}^H \mathbf{y}_{i,f,t} = \mathbf{\Lambda}_{i,f,t} \mathbf{D}_{i,f,t} \mathbf{x}_{i,f,t} + \mathbf{n}'_{i,f,t} \quad (9)$$

where $\mathbf{n}'_{i,f,t} \in \mathbb{C}^{n_B^{(i)} \times 1}$ has covariance $\sigma_i^2 \mathbf{I}$ and is approximated to be standard complex AWGN. The post-equalization SINR $\rho_{i,j,f,t}$ for the j^{th} received symbol of UE i , $i \in \mathcal{I}_{f,t}$ on RE (f,t) is

$$\rho_{i,j,f,t} = \lambda_{i,j,f,t} p_{i,j,f,t} / \sigma_i^2. \quad (10)$$

C. Expected UE Rates

Modern communication systems use bit-interleaved coded modulation (BICM) [10] where, due to the usage of scrambling and interleaving, the transmitted bits in an RE are approximately independent and identically distributed. Let $\mathcal{G}_i \triangleq \{(f,t) | i \in \mathcal{I}_{f,t}\}$ denote the indices of the RE allocated for communication between the BS and UE i . In practical communication systems, there is finite number of modulation and coding schemes (MCSs). For example, 5G NR Table 2 supports up to 27 MCS levels [8, Table 5.1.3.1-2], with the lowest level using 4-QAM and a rate- $\frac{120}{1024}$ low-density parity-check (LDPC) code with spectral efficiency (SE) given by $(120/1024) \log_2(4) = 0.234$, and the highest level using 256-QAM and a rate- $\frac{948}{1024}$ LDPC code with SE $(948/1024) \log_2(256) = 7.40$. We denote the minimum MCS SE by r_{min} and the maximum SE possible by $r_{max} = \log_2(|Q_{max}|)$, respectively, where Q_{max} is the highest-order constellation used in the system. The achievable rate $R_{UE,i}$ (in bits per slot) for UE i is upper-bounded as

$$R_{UE,i} \leq \sum_{(f,t) \in \mathcal{G}_i} \sum_{j=1}^{n_l^{(i)}} I_{Q_i}(\rho_{i,j,f,t}) \quad (11)$$

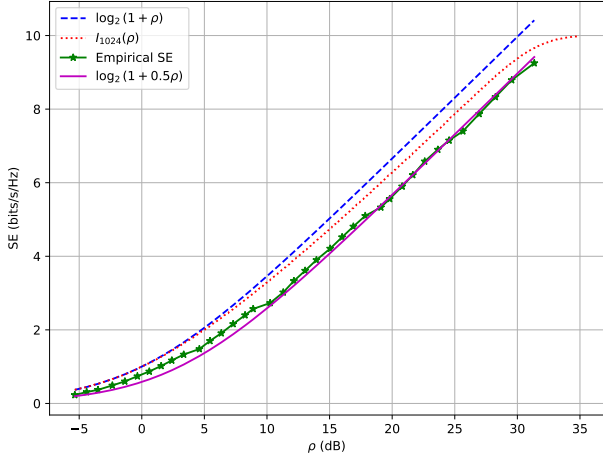


Fig. 1. Comparison between the plots of SE vs. SNR for different functions.

where $\rho_{i,j,f,t,i}$ is the post-equalization SINR for the j^{th} received symbol of UE i in the RE indexed by (f,t) , and $I_Q(x)$ refers to the mutual-information (MI) between the input and the output in an AWGN channel for constellation Q and an SNR of x . Since there is a minimum MCS SE r_{min} , reliable communication is not guaranteed if the expression in (11) is lower than $|\mathcal{G}_i| n_l^{(i)} r_{min}$. Therefore, the achievable rate for UE i is

$$R_{UE,i} = x \mathbb{I}_{\{x > n_l^{(i)} |\mathcal{G}_i| r_{min}\}} \quad (12)$$

where x where is given by the R.H.S. of (11).

III. THE JOINT RESOURCE-POWER ALLOCATION AND UE RANK SELECTION PROBLEM

For casting the joint resource-power allocation and UE rank selection as an optimization problem, we first need to obtain a suitable differentiable function that well-approximates $I_{Q_{max}}(\cdot)$ in (11), where Q_{max} is the highest-order constellation used. Fig. 1 plots the SE as a function of SNR, denoted by ρ , for four functions; $\log_2(1+\rho)$ is the Shannon capacity, $I_{1024}(\rho)$ refers to the empirically-obtained mutual information between the input and output of an AWGN channel with 1024-QAM, ‘‘Empirical SE’’ refers to the empirically obtained set of values of SNRs required to achieve a codeword error rate (CER) of 10^{-3} in a single-input single-output (SISO) AWGN channel for each MCS level of the combined tables of [8, Tables 5.1.3.1-2, 5.1.3.1-4] using 5G NR LDPC codes of length 2880. As evident from the figure, the Shannon capacity is an overly optimistic approximation for practical communication systems that use finite-sized constellations (e.g., 2^m -QAM) while $I_{1024}(\rho)$ is still too optimistic for systems that use practical error-correcting codes. A good approximation needs to be conservative for lower MCS indices due to the fact that lower MCS levels serve UEs that have relatively low SINR, and $\log_2(1+0.5\rho)$ is one such logarithmic approximation that is closer to practical rates than the theoretical mutual information. We would like to emphasize that $\log_2(1+0.5\rho)$ is just an exemplary function that will be used in the rest of this paper, and better differentiable functions can be obtained by suitable optimization.

As mentioned in the previous section, the BS needs to have reasonably good channel estimates to perform resource-power allocation. These channel estimates are not available for each PRB, but for groups of PRBs which we call PRBG in this paper. Let n_{PRB} denote the total number of PRBs and n_{RBG} the total number of PRBGs in the system so that we have a channel estimate for every n_{PRB}/n_{RBG} PRBs. Let $\delta_{i,g} \in \{0, 1\}$ indicate whether PRBG g is allocated to UE i ($\delta_{i,g} = 1$) or not ($\delta_{i,g} = 0$). Note that unlike in 5G NR, we do not restrict the frequency allocation to be contiguous in this paper. For every notation used in Section II, we use the subscript g instead of (f,t) to denote that the notation applies to PRBG g instead of RE (f,t) . With this, the BS uses the channel estimates to obtain estimates of the SINR $\rho_{i,j,g}$ for the j^{th} symbol of UE i on PRBG g using (5) for the uplink and (10) for the downlink, where, for the latter, the BS uses the interference-plus-noise variance feedback from each UE. Henceforth, we use the notation $\mathcal{G} \triangleq \{1, \dots, n_{RBG}\}$, $\mathcal{N}_{UE} \triangleq \{1, \dots, N_{UE}\}$.

Let $R_{UE,i}$ denote the normalized (with respect to some constant) rate in bits per slot for UE i . It is a common practice to maximize a weighted α -fair utility function [11] $\sum_{i=1}^{N_{UE}} a_i f_\alpha(R_{UE,i})$, where $f_\alpha(\cdot)$, $\alpha > 0$, is an increasing, strictly concave, and continuously differentiable function on the open interval $(0, \infty)$, as follows:

$$f_\alpha(x) = \begin{cases} \frac{x^{1-\alpha}}{1-\alpha}, & \text{if } \alpha > 0, \alpha \neq 1, \\ \ln(x), & \text{if } \alpha = 1. \end{cases} \quad (13)$$

Here, the weights satisfy $a_i > 0, \forall i$. In this paper, we take $a_i = 1, \forall i \in \mathcal{N}_{UE}$ and $\alpha = 1$, which corresponds to the *geometric mean (GM) rate optimization or proportional fairness* [12]. However, our problem formulation is applicable to any value of α .

A. Uplink Joint Resource-power Allocation and UE Rank Selection

The BS obtains the channel estimates $\hat{\mathbf{H}}_{i,g} \in \mathbb{C}^{n_B \times n_l^{(i)}}$ corresponding to the first $n_l^{(i)}$ columns of $\mathbf{R}_g^{-1/2} \mathbf{H}_{i,f,t} \mathbf{W}_{i,f,t}$ of Section II-A for PRBG g (note that the interference-plus-noise covariance is now calculated at the PRBG level and not at the RE level). Let $\hat{\mathbf{H}}_g \triangleq [\hat{\mathbf{H}}_{1,g}, \dots, \hat{\mathbf{H}}_{N_{UE},g}] \in \mathbb{C}^{n_B \times n_L}$ where $n_L = \sum_{i=1}^{N_{UE}} n_l^{(i)}$. Then, with transmit powers $p_{i,j,g} > 0, j = 1, \dots, n_l^{(i)}$, for UE i on PRBG g , we get an SINR of $\rho_{i,j,g} = \lambda_{i,j,g} p_{i,j,g}$ for a hypothetically transmitted j^{th} layer of UE i on PRBG g , where $\lambda_{i,j,g}$ is the reciprocal of the $(\sum_{i'=1}^{i-1} n_l^{(i')} + j)^{\text{th}}$ diagonal element of $[\hat{\mathbf{H}}_g^H \hat{\mathbf{H}}_g]^{-1}$. Therefore, from the log approximation function $\log_2(1+0.5\rho)$, the normalized expected rate in bits per slot (normalized by T times the number of subcarriers in a PRBG) for UE i is given by

$$R_{UE,i} = \sum_{g=1}^{n_{RBG}} \sum_{j=1}^{n_l^{(i)}} \log_2(1+0.5\delta_{i,g}\lambda_{i,j,g}p_{i,j,g}). \quad (14)$$

Let ρ_{max} correspond to the SNR required to achieve a SE of r_{max} , i.e., $\rho_{max} = 2(2^{r_{max}} - 1)$. With this, the goal of the

resource allocation problem is to maximize the GM of the UE rates, or equivalently, $\sum_{i=1}^{N_{UE}} \ln(R_{UE,i})$, as follows:

P_{UL} :

$$\max_{p_{i,j,g}, \delta_{i,g}, n_l^{(i)}} \sum_{i=1}^{N_{UE}} \ln(R_{UE,i}) \quad (15a)$$

$$\text{s.t.} \quad \delta_{i,g} \in \{0, 1\}, \sum_{g \in \mathcal{G}} \delta_{i,g} \geq 1, \forall i, g, \quad (15b)$$

$$n_l^{(i)} \leq n_U^{(i)}, \forall i, \quad (15c)$$

$$0 \leq p_{i,j,g} \leq \rho_{max}/\lambda_{i,j,g}, \forall i, \forall g, \forall j, \quad (15d)$$

$$R_{UE,i} \geq r_{min} n_l^{(i)} \sum_{g \in \mathcal{G}} \delta_{i,g}, \forall i, \quad (15e)$$

$$\sum_{g \in \mathcal{G}} \sum_{j=1}^{n_l^{(i)}} \delta_{i,g} p_{i,j,g} \leq P_{U,max}, \forall i. \quad (15f)$$

In the above optimization problem, (15b) imposes an allocation requirement of at least one PRBG for each UE but any arbitrary value $n_{RBG,min} \geq 1$ is possible. Also, (15d) can be replaced by a UE-specific maximum power that would cater to power allocation for UEs with different quality-of-services (QoSs), or to limit the ICI. **In the latter case, ρ_{max} is the equivalent of (P_0, α) for uplink power control** (see Section V-A). The constraint in (15e) is a reformulation of (12).

B. Downlink Joint Resource-power Allocation and UE Rank Selection

The setup is as described in Section II-B with the usage of notation and the PRBG indices in the subscripts of symbols as explained in Section III-A. Without loss of generality, we assume that $\sigma_i^2 = 1, \forall i = 1, \dots, N_{UE}$, so that from (10), the normalized expected rate in bits per slot (normalized by T times the number of subcarriers in a PRBG) for UE i is the same as in (14). The resource allocation problem P_{DL} can now be expressed as

P_{DL} :

$$\max_{p_{i,j,g}, \delta_{i,g}, n_l^{(i)}} \sum_{i=1}^{N_{UE}} \ln(R_{UE,i}) \quad (16a)$$

$$\text{s.t.} \quad \delta_{i,g} \in \{0, 1\}, \sum_{g \in \mathcal{G}} \delta_{i,g} \geq 1, \forall i, \forall g, \quad (16b)$$

$$n_l^{(i)} \leq n_U^{(i)}, \forall g, \quad (16c)$$

$$0 \leq p_{i,j,g} \leq \rho_{max}/\lambda_{i,j,g}, \forall i, \forall g, \forall j, \quad (16d)$$

$$R_{UE,i} \geq r_{min} n_l^{(i)} \sum_{g \in \mathcal{G}} \delta_{i,g}, \forall i, \quad (16e)$$

$$\sum_{k=1}^{n_B} \sum_{i=1}^{N_{UE}} \sum_{j=1}^{n_l^{(i)}} \sum_{g \in \mathcal{G}} \delta_{i,g} a_{k,i,j,g} p_{i,j,g} \leq P_{B,max}, \quad (16f)$$

$$\sum_{i=1}^{N_{UE}} \sum_{j=1}^{n_l^{(i)}} \sum_{g \in \mathcal{G}} \delta_{i,g} a_{k,i,j,g} p_{i,j,g} \leq P_{ant}, \forall k. \quad (16g)$$

Except for the expressions for the post-equalization SINR, the only other significant difference between the problem formulations P_{UL} and P_{DL} is that for the downlink, the available BS transmit power needs to be shared by all the UE as shown in (16f), and that there is also an additional PAPC at the BS as shown in (16g).

Both P_{UL} and P_{DL} are non-convex optimization problems and involve mixed integer programming. It is possible that there exists no unique optimal solution, or that an optimal solution cannot be obtained without too many iterations. In the next section, we propose a method to obtain a reasonably good (even if possibly sub-optimal) solution to the two problems without too many iterations.

IV. THE PROPOSED OPTIMIZATION TECHNIQUE

SINR estimation as given by (5) and (10) requires computationally intensive matrix inversions, potentially involving Moore-Penrose inversion, singular value decomposition (SVD) or eigenvalue decomposition (EVD) depending on the ZF-precoding type used [1]. Since P_{UL} and P_{DL} are both non-convex, there is no guarantee that any proposed approach might lead to an optimal solution. Hence, the goal is to obtain a possibly sub-optimal solution without incurring a high computational complexity. In this regard, we split both optimization problems into two convex optimization stages with an intermediate processing stage in between. In lieu of P_{UL} and P_{DL} , we consider the following problems where $\delta_{i,g}$ and $n_l^{(i)}$ are fixed and not optimized over:

\bar{P}_{UL} :

$$\min_{p_{i,j,g}} - \sum_{i=1}^{N_{UE}} \ln(R_{UE,i}) \quad (17a)$$

$$\text{s.t.} \quad 0 \leq p_{i,j,g} \leq \rho_{max}/\lambda_{i,j,g}, \forall i, \forall g, \forall j, \quad (17b)$$

$$\sum_{g=1}^{n_{RBG}} \sum_{j=1}^{n_l^{(i)}} \delta_{i,g} p_{i,j,g} \leq P_{U,max}, \forall i \in N_{UE}, \quad (17c)$$

for the uplink, and

\bar{P}_{DL} :

$$\min_{p_{i,j,g}} - \sum_{i=1}^{N_{UE}} \ln(R_{UE,i}) \quad (18a)$$

$$\text{s.t.} \quad 0 \leq p_{i,j,g} \leq \rho_{max}/\lambda_{i,j,g}, \forall i, \forall g, \forall j, \quad (18b)$$

$$\sum_{k=1}^{n_B} \sum_{i=1}^{N_{UE}} \sum_{j=1}^{n_l^{(i)}} \sum_{g=1}^{n_{RBG}} \delta_{i,g} a_{k,i,j,g} p_{i,j,g} \leq P_{B,max}, \quad (18c)$$

$$\sum_{i=1}^{N_{UE}} \sum_{j=1}^{n_l^{(i)}} \sum_{g=1}^{n_{RBG}} \delta_{i,g} a_{k,i,j,g} p_{i,j,g} \leq P_{ant}, \forall k, \quad (18d)$$

for the downlink. Also to note is that the non-convex constraints (15e) and (16e) are not considered. With this, both \bar{P}_{UL} and \bar{P}_{DL} are now convex-optimization problems with convex objectives and affine constraints and can be solved using interior point methods [13] for which there exist efficient

large-scale optimization software like Interior Point OPTimizer (IPOPT) [14]. Let $\text{OPT} \left(\bar{P} \left(\left\{ \lambda_{i,j,g}, \delta_{i,g}, n_l^{(i)}, \forall i, j, g \right\} \right) \right)$ denote the solution to the convex optimization problem \bar{P} , where \bar{P} is either \bar{P}_{UL} or \bar{P}_{DL} as the case may be. Further, we denote by $f \left(\hat{\mathbf{H}}_g, \left\{ \delta_{i,g}, n_l^{(i)}, \forall i \in \mathcal{N}_{UE} \right\} \right)$ the set of values $\lambda_{i,j,g}, \forall i, j, g$. Note that for the uplink (see Sec. III-A), $\lambda_{i,j,g}$ is the reciprocal of the $(\sum_{i'=1}^{i-1} n_l^{(i')} + j)^{th}$ diagonal element of $[\hat{\mathbf{H}}_g^H \hat{\mathbf{H}}_g]^{-1}$, while for the downlink, it is obtained from the product of the channel matrix and the ZF precoder (see Sec. II-B). In both cases, $\lambda_{i,j,g}$ depends on the set of UEs that share the PRBG and the number of layers for each such UE. Therefore, we add the following definition, $\forall i \in \mathcal{N}_{UE}, \forall g \in \mathcal{G}$:

$$\lambda_{i,j,g} = 0, \forall j \in \left\{ 1, \dots, n_U^{(i)} \mid \delta_{i,g} = 0 \right\}, \quad (19)$$

$$\lambda_{i,j,g} = 0, n_l^{(i)} < j \leq n_U^{(i)}. \quad (20)$$

Since the optimization problems P_{UL} and P_{DL} are similarly structured, we now provide a unified approach for the joint resource-power allocation and UE rank selection for both the uplink and the downlink. In the first stage, we propose to fix $\delta_{i,g} = 1, n_l^{(i)} = n_U^{(i)}, \forall i \in \mathcal{N}_{UE}, \forall g \in \mathcal{G}$, and solve $\bar{P} = \bar{P}_{UL}$ or \bar{P}_{DL} as the case may be. Let $\left\{ p_{i,j,g}^{(1)}, j = 1, \dots, n_U^{(i)}, \forall i \in \mathcal{N}_{UE}, \forall g \in \mathcal{G} \right\} = \text{OPT} \left(\bar{P} \left(\left\{ \lambda_{i,j,g}, \delta_{i,g} = 1, n_l^{(i)} = n_U^{(i)}, \forall i, j, g \right\} \right) \right)$ be the solution obtained in Stage 1.

The details of the second stage are better explained using Algorithm 1. Steps 9–10 identify the weak PRBGs and layers for each UE. Next, the idea is to start conservatively at $n_l^{(i)} = 1$ layer for each UE and check iteratively if additional layers can be accommodated. Steps 11–16 perform these operations, noting that the number of layers remains constant across all allocated PRBGs for each UE. Step 13 is used to ensure that (15e) or (16e) is respected. Once the number of layers has been identified for each UE, the next check is to ensure that the minimum number of PRBGs $n_{RBG,min}$ is assigned to each UE. If not, Steps 20–21 assign the PRBGs with the $n_{RBG,min}$ highest values of estimated UE rates for the UE in context. Finally, once the PRBG allocation and UE ranks have been arrived at, the values of $\lambda_{i,j,g}$ are recalculated in Step 27 if there is a change in the PRBG allocation and the UE ranks with respect to Stage 1, keeping also in mind (19) and (20). Step 28 ensures that the PRBGs that are not allocated and the UE layers that are not selected will play no further part in the optimization. If each UE is *servable* (i.e., it is possible to guarantee a minimum rate for that UE for some feasible resource-power allocation), by choosing to maximize the GM rates and due to Steps 11–16, we would have already ensured that the finally allocated PRBGs and layers for each UE are such that each UE has a minimum rate guarantee in the slot. Next, with $\rho_{min} \triangleq 2(2^{r_{min}} - 1)$, we set the lower limit on $p_{i,j,g}$ in (17b) and (18b) to $\rho_{min}/\lambda_{i,j,g}$ if $\delta_{i,g}^* = 1$ and $j = 1, \dots, n_l^{(i)}$, and 0 otherwise. Then, the output of Step 27 provides the final allocated powers to each layer and each PRBG for each UE.

Remark 1. *If there is a non-servable UE, (i.e., a UE with*

Algorithm 1 Pseudocode for MU-MIMO resource-power allocation and UE rank selection.

```

1: Output
2:  $\delta_{i,g}^*$  : PRBG  $g$  allocation indicator for UE  $i, \forall i \in \mathcal{N}_{UE}, \forall g \in \mathcal{G}$ 
3:  $n_l^{(i)}$  : The assigned rank for UE  $i, \forall i \in \mathcal{N}_{UE}$ 
4:  $p_{i,j,g}^*$  : The allocated powers,  $j = 1 \dots, n_U^{(i)}, \forall i \in \mathcal{N}_{UE}, \forall g \in \mathcal{G}$ 
5:  $\delta_{i,g} \leftarrow 1, n_l^{(i)} \leftarrow n_U^{(i)}, \forall i \in \mathcal{N}_{UE}, \forall g \in \mathcal{G}$ 
6:  $\lambda_{i,j,g} \leftarrow f \left( \hat{\mathbf{H}}_g, \left\{ \delta_{i,g}, n_l^{(i)}, \forall i \in \mathcal{N}_{UE} \right\} \right), \forall i \in \mathcal{N}_{UE}, \forall g \in \mathcal{G}$ 
7:  $\left\{ p_{i,j,g}^{(1)}, \forall i, j, g \right\} \leftarrow \text{OPT} \left( \bar{P} \left( \left\{ \lambda_{i,j,g}, \delta_{i,g}, n_l^{(i)}, \forall i, j, g \right\} \right) \right)$ 
8: for all  $i \in \mathcal{N}_{UE}$  do
9:    $r_{i,j,g} \leftarrow \log_2 \left( 1 + 0.5 \lambda_{i,j,g} p_{i,j,g}^{(1)} \right), \quad \forall j = 1, \dots, n_U^{(i)}, \forall g \in \mathcal{G}$ 
10:   $\delta_{i,j,g} \leftarrow 1$  if  $r_{i,j,g} \geq r_{min}$ , 0 otherwise,  $\forall j = 1, \dots, n_U^{(i)}, \forall g \in \mathcal{G}$ 
11:   $r_{current} \leftarrow 0, r_{mean} \leftarrow 0, n_l^{(i)} \leftarrow 1$ 
12:   $\delta_{i,g} \leftarrow \prod_{j=1}^{n_l^{(i)}} \delta_{i,j,g}, \forall g \in \mathcal{G}$ 
13:   $r_{i,sum} \leftarrow \sum_{g=1}^{n_{RBG}} \delta_{i,g} \sum_{j=1}^{n_l^{(i)}} r_{i,j,g}, r_{i,mean} \leftarrow r_{i,sum} / \left( n_l^{(i)} \sum_{g=1}^{n_{RBG}} \delta_{i,g} \right)$ 
14:  if  $r_{i,sum} > r_{current}$  &  $r_{i,mean} > r_{min}$  &  $n_l^{(i)} < n_U^{(i)}$  then
15:     $n_l^{(i)} \leftarrow n_l^{(i)} + 1$ 
16:  go to 12
17:  else
18:    if  $\sum_{g \in \mathcal{G}} \delta_{i,g} < n_{RBG,min}$  then
19:      /* Identify a set  $\mathcal{A}_i$  of PRBGs with the  $n_{RBG,min}$  highest values of UE rates */
20:       $\mathcal{A}_i \leftarrow \arg \max_{\mathcal{A} \subset \mathcal{G}, |\mathcal{A}| = n_{RBG,min}} \left\{ \sum_{g \in \mathcal{A}} \sum_{j=1}^{n_l^{(i)}} r_{i,j,g} \right\}$ 
21:       $\delta_{i,g}^* \leftarrow 1, \forall g \in \mathcal{A}_i$ , and  $\delta_{i,g}^* \leftarrow 0, \forall g \notin \mathcal{A}_i$ 
22:    else
23:       $\delta_{i,g}^* \leftarrow \delta_{i,g}$ 
24:    end if
25:  end if
26: end for
27:  $\lambda_{i,j,g} \leftarrow f \left( \hat{\mathbf{H}}_g, \left\{ \delta_{i,g}^*, n_l^{(i)}, \forall i \in \mathcal{N}_{UE} \right\} \right), \quad \forall j = 1, \dots, n_U^{(i)}, \forall i \in \mathcal{N}_{UE}, \forall g \in \mathcal{G}$ 
28:  $\left\{ p_{i,j,g}^*, \forall i, j, g \right\} \leftarrow \text{OPT} \left( \bar{P} \left( \left\{ \lambda_{i,j,g}, \delta_{i,g}^*, n_l^{(i)}, \forall i, j, g \right\} \right) \right)$ 

```

extremely poor channel conditions for which no allocations are possible to guarantee a minimum rate in the slot in context), such a UE would adversely affect the optimization problem. A prudent approach would be to not serve this UE at all in the first place until its channel conditions improve.

A. Uplink Scheduling Information

Having obtained the UE transmit powers, the UE ranks, and the resource allocation indices, the BS must now transmit this information to each co-scheduled UE on a downlink control information (DCI) [15] message. However, the standard DCI

formats in 5G NR can only encode a single low-resolution closed-loop power control command per UE and slot. Instead, the MU-MIMO power-control solution we propose requires transmit power control (TPC) commands that are PRBG-, slot-, and layer-specific. 5G NR DCI formats are therefore insufficient to convey these data-rich BS decisions. For this reason, we propose the following additional features to support MU-MIMO TPC commands. Note that these features differ in the amount of signaling overhead, and consequently, not all of them may be preferred in all scenarios.

- 1) *High granularity DCI*: The DCI encodes the discretized full set of transmit powers for each PRBG on each layer. This incurs the highest overhead and might be practical in 6G deployments with extreme bandwidths.
- 2) *Medium granularity DCI*: A condensed set of discretized transmit powers, only one per layer, is sent. In this case, the UE uses the same transmit power for all scheduled PRBGs per layer. This embodiment may yield the best trade-off between performance and signaling overhead, and it may be optimal in deployments with low-frequency selectivity, such as rural outdoors.
- 3) *Low granularity DCI*: A single discretized transmit power per UE is transmitted on the DCI. In this case, the UE uses a common transmit power for all the scheduled PRBs and layers. This incurs the least overhead, and depending on the case, might not significantly degrade the performance compared to the having separate transmit powers per PRBG and layer.

B. Possible Limitations of the proposed technique

The performance of the proposed technique hinges entirely on the accuracy of channel estimates $\hat{\mathbf{H}}_g, \forall g \in \mathcal{G}$. As a result, one can expect it to break down under one or more of the following scenarios.

If the BS-UE communication is FDD, the uplink channel is unlikely to be the reciprocal of the downlink channel and it would not be realistic to use the proposed technique for the downlink if the channel estimates are obtained from the uplink SRS. However, if the UE were to feedback the downlink channel that it estimates, for example, using channel-state information reference signals (CSI-RSs) [8, Section 7.4.1.5], the proposed technique can be still employed.

If some of the UEs have poor channel conditions (e.g., cell-edge UEs) and an insufficient power budget to ensure a certain SINR at the BS, the BS would not be able to obtain good quality channel estimates from the SRSs of these UEs. This scenario would adversely impact the downlink more because the assumed ZF precoder design would no longer be valid.

C. Computational Complexity and Practical Considerations

Interior-point methods solve the following convex optimization problem in its standard form [14]:

$$\min_{\mathbf{x} \in \mathbb{R}^n} f(\mathbf{x}) \quad (21a)$$

$$\text{subject to} \quad \mathbf{c}_L \leq \mathbf{c}(\mathbf{x}) \leq \mathbf{c}_U, \quad (21b)$$

$$\mathbf{x}_L \leq \mathbf{x} \leq \mathbf{x}_U, \quad (21c)$$

where $\mathbf{x}_L \in [-\infty, \infty)^n$, $\mathbf{x}_U \in (-\infty, \infty]^n$ with $[\mathbf{x}_L]_i < [\mathbf{x}_U]_i$, $\forall i = 1, \dots, n$, $\mathbf{c}_L \in [-\infty, \infty)^m$, $\mathbf{c}_U \in (-\infty, \infty]^m$ with $[\mathbf{c}_L]_i < [\mathbf{c}_U]_i$, $\forall i = 1, \dots, m$. The objective function is $f: \mathbb{R}^n \rightarrow \mathbb{R}$ and the constraint function is $c: \mathbb{R}^n \rightarrow \mathbb{R}^m$ (with any equality constraint being set by choosing $\mathbf{c}_L = \mathbf{c}_U$). For a tolerance $\epsilon > 0$, the number of required iterations to obtain a solution is $\mathcal{O}(\sqrt{n} \ln(1/\epsilon))$ [16]. Further, each iteration involves solving a linear system of equations that has a worst-case complexity of $\mathcal{O}(n^3)$. Note that this is an upper bound and dependent on the form of the objective function and how entangled the variables are with one another, and most practical linear solvers have a complexity less than $\mathcal{O}(n^3)$. Nevertheless, the worst-case complexity of any interior-point method in order to achieve a tolerance of $\epsilon > 0$ is $\mathcal{O}(n^{3.5} \ln(1/\epsilon))$.

The proposed technique uses two optimization stages with each optimization stage solving a convex optimization problem with $n = n_{RBG}n_U$ variables where $n_U = \sum_i n_U^{(i)}$. For the uplink problem (17a), the nature of the objective and the constraints imply that the optimization for each UE can be done separately. So, this translates to solving N_{UE} independent optimization problems with $n = n_{RBG}n_U^{(i)}$ variables for UE i in the first stage and $n = n_{RBG}n_U^{(i)}$ variables in the second stage. But each stage of the proposed technique requires the computation of $[\hat{\mathbf{H}}_g^H \hat{\mathbf{H}}_g]^{-1}$, $\forall g = 1, \dots, n_{RBG}$, where $\hat{\mathbf{H}}_g \in \mathbb{C}^{n_B \times n_U}$, which has a worst-case complexity of $\mathcal{O}(n_{RBG}n_U^3)$. So, the worst-case complexity of the proposed technique for the uplink is $\mathcal{O}(N_{UE}(n_{RBG}n_{U,max})^{3.5} \ln(1/\epsilon) + n_{RBG}n_U^3)$, where $n_{U,max} = \max_{i \in N_{UE}} \{n_U^{(i)}\}$.

For the downlink, all the $n = n_{RBG}n_U$ variables need to be jointly optimized, leading to a worst-case complexity of $\mathcal{O}((n_{RBG}n_U)^{3.5} \ln(1/\epsilon))$. Note that while the ZF precoders need to be calculated in order to obtain the $\lambda_{i,j,g}$, this is anyway unavoidable for downlink transmission and hence not part of the additional complexity resulting from the usage of the proposed technique. Further, note that since the Hessian of the objective function as shown in (18a) allows a block-diagonal structure, each iteration of the optimization problem involves solving a sparse linear system of equations which significantly reduces the overall complexity. If PRBG allocation is not considered, i.e., all the available PRBGs are allocated to every UE, the complexity is significantly reduced from $\mathcal{O}((n_{RBG}n_U)^{3.5} \ln(1/\epsilon))$ to $\mathcal{O}(n_U^{3.5} \ln(1/\epsilon))$, but this might come at the cost of throughput performance, especially in highly frequency selective channels. Further, we can always neglect the requirement on a certain error tolerance and fix the number of iterations to a predetermined number. This would further tradeoff performance for lower complexity.

The computational burden of our method, requiring the execution of IPOPT every slot, presents a substantial challenge for real-time 6G implementation. To address this, we propose investigating both supervised and reinforcement learning approaches. Supervised learning could involve training a model on a dataset for which the labels have been obtained by the proposed technique, allowing for rapid prediction in subse-

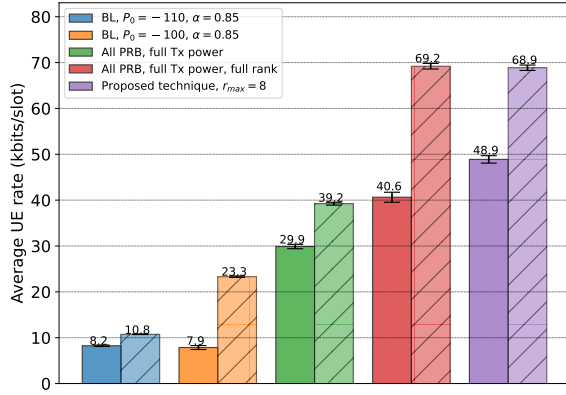


Fig. 2. UL: Plots (with 90% confidence interval) of the UE GM rates (plain bar) and AM rates (hatched bars) in bits/slot for the isolated cell case.

quent slots. Alternatively, reinforcement learning, guided by our proposed technique as an expert policy, could uncover even better performing methods. Future research will focus on exploring these ML-based techniques, aiming to balance computational efficiency and performance.

V. SIMULATION RESULTS

We consider the following setup (with a summary of the parameters in Table I) for performing multi-cell, multi-link-level simulations, the code for which was written in NumPy (for channel generation) and TensorFlow. We consider 7 sites with 3 cells per site, leading to a total of 21 cells arranged in a hexagonal grid with wraparound (which essentially means that each cell sees an ICI pattern similar to that of the central cell). Each cell serves only at most 8 UEs per slot in MU-MIMO mode. We consider the following two scenarios:

- 1) All the cells are isolated which means that there is no ICI. This corresponds to the case $\mathbf{R}_{f,t} = \sigma^2 \mathbf{I}$ in (3), where σ^2 is the thermal noise variance.
- 2) Cells with ICI from the adjacent cells whose statistics vary from slot to slot depending on the paired UEs in the adjacent cells. In this case, there is no way of obtaining an accurate enough estimate of \mathbf{R}_g (introduced in Section III-A) at the BS in order to accurately estimate the correct MCS for all the co-scheduled UEs unless the ICI is lower than or comparable to the thermal noise level.

For the uplink, we use QPSK, 16-QAM, 64-QAM, and 256-QAM while for the downlink, we also use 1024-QAM. Explicit data transmission, receiver equalization, and channel coding/decoding using 5G NR LDPC codes are performed. We assume the availability of perfect CSI but no open loop link-adaptation (OLLA) [17] or hybrid automatic repeat request (HARQ) whose inclusion, in practice, can be expected to make up for ill-effects of imperfect CSI. Therefore, MCS selection is done as detailed in [18] while taking \mathbf{R}_g to be $\sigma^2 \mathbf{I}$ in (3), where σ^2 is the thermal noise variance per PRB.

TABLE I
A LIST OF SIMULATION PARAMETERS.

| Parameter | Value |
|--------------------------------------|--|
| N_{UE} | 8 (maximum) |
| $n_U^{(i)}$ | 4 ($2H \times 1V \times 2P$), $\forall i$ |
| n_B | 128 ($4H \times 16V \times 2P$) |
| Number of cells in the network | 21 |
| Total number of UEs in the network | 210 |
| Inter-site distance | 500 m |
| Channel model | 38.901 Urban Macro (UMa) NLoS |
| Carrier frequency | 3.5 GHz |
| OFDM subcarrier spacing | 30 kHz |
| T | 14 |
| Slot duration | 0.5 ms |
| Bandwidth | 8.64 MHz (24 PRBs) |
| n_{RBG} | 24 (1 PRB per PRBG) |
| $n_{RBG,min}$ | 4 (uplink), 2 (downlink) |
| $P_{B,max}$ | 36 dBm for 8.64 MHz |
| UE speed | 3 kmph |
| $P_{U,max}$ | 23 dBm for 8.64 MHz |
| UE OLPC parameters (P_0, α) | P_0 (dBm) $\in \{-85, -90, -100, -110\}$, $\alpha \in \{0.85, 1\}$ |
| Channel coding | 5G NR LDPC [15, Section 5.3.2] with rate-matching |
| Channel estimation | Perfect CSI |
| MCS | Table 5.1.3.1-2 (uplink), Table 5.1.3.1-4 (downlink) of [8] |
| Scheduler | Plain Round Robin |
| HARQ | No |
| Number of independent UE drops | 10 |
| Number of slots per drop | 100 |
| Receiver equalizer | LMMSE |
| Downlink precoder | Block diagonalization ZF [1] |
| CSI acquisition frequency | Once every 20 slots |
| Number of iterations of IPOPT | 10 |

A. Uplink Results

Baseline power control: The total transmit power P_i (dBm) for UE i is obtained by setting the OLPC parameters (P_0, α) in the following [19, Section 7]:

$$P_i = \min\{P_{U,max}, P_0 + 10 \log_{10}(n_{PRB,i}) + \alpha PL_i\} \quad (22)$$

where $P_{U,max} = 23$ dBm for the bandwidth considered, $n_{PRB,i} \in [4, 24]$ is the total number of PRBs assigned to UE i , PL_i is the pathloss estimate (based on the measured channel gains on the downlink), P_0 (dBm) is the expected received power per PRB under full pathloss compensation, and $\alpha \in [0, 1]$ is the fractional pathloss compensation factor.

Baseline PRBG allocation: We assume that all the PRBGs are allocated to the UE unless power-limited. In the latter case, we assign a number of PRBGs (subject to a minimum of 4) over which the UE has sufficient power to transmit, choosing the available PRBGs with the strongest channel gains for that UE.

Baseline UE rank selection: Let the channel covariance (at the UE) for UE i be $\mathbf{R}_{h,UE}^{(i)} \triangleq \mathbb{E}_{f,t} [\mathbf{H}_{i,f,t}^H \mathbf{H}_{i,f,t}] \in \mathbb{C}^{n_U^{(i)} \times n_U^{(i)}}$ with ordered eigenvalues $\mu_1 \geq \mu_2 \geq \dots \geq \mu_{n_U^{(i)}}$. The UE rank $n_l^{(i)}$ for the baseline scheme is taken to be $n_l^{(i)} =$

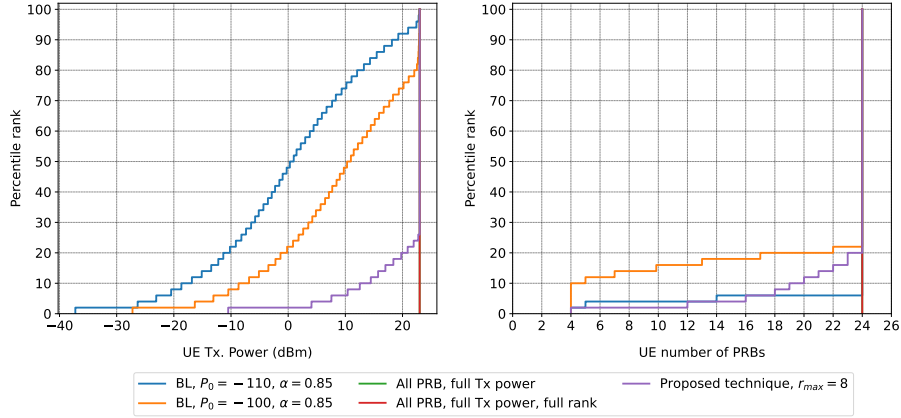


Fig. 3. UL: Percentile ranks of the UE transmit power (left) and the PRB allocation for the isolated cell case.

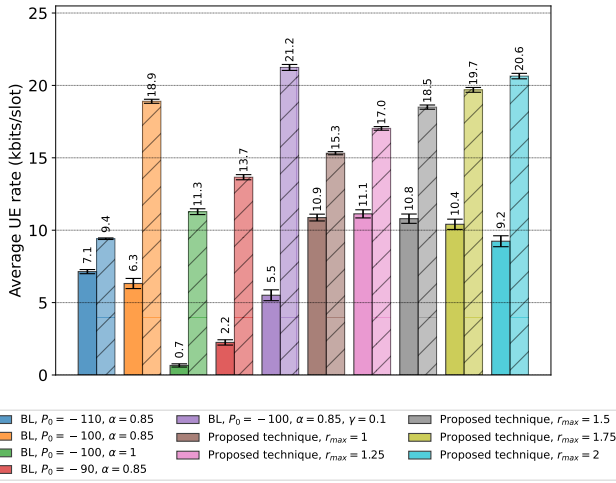


Fig. 4. UL: Plots (with 90% confidence interval) of the UE GM rates (plain bar) and AM rates (hatched bars) in bits/slot with ICI.

$\max \left\{ n \in \{1, \dots, n_U^{(i)}\} \mid \mu_n / \mu_1 \geq \gamma \right\}$ where $\gamma \in (0, 1]$ is a predefined threshold and taken to be 0.5, 0.1, or 0.01 in this study. Further, $n_l^{(i)} = 1$ if $n_{RBG,i} = n_{RBG,min}$.

Apart from these baseline schemes, we also consider the case where all the PRBs are allocated to all the UEs with full transmit power and also with full rank ($n_l^{(i)} = n_U^{(i)}, \forall i$). For the proposed scheme, Algorithm 1 is executed but a *uniform transmit power across layers and PRBs is applied by taking the mean of the obtained PRB-wise and layer-wise powers for the UE in context*.

Fig. 2 shows the comparison (“BL” indicates “baseline”) of the average GM and arithmetic mean (AM) UE rates, both computed per slot and then averaged across slots and independent UE drops. While the proposed technique is not targeted at maximizing the AM rates, they have been shown purely for illustration. Since there is no ICI, it is obvious that aggressively using as much of the available transmit power as required is generally the best strategy. Therefore, we use $r_{min} = 0.23$ (corresponding to 4-QAM with the least coding rate in 5G NR) and $r_{max} = 8$ (corresponding to the upper bound on the rate per data symbol for 256-QAM) for

the proposed technique (Section III-A). While the proposed technique not only achieves the best GM UE rates, it also does so while requiring lower UE transmit powers than the naive, full transmit power scheme, as shown in Fig. 3.

For the case with ICI, since the transmit powers of the served UEs affect the reception in the neighbouring cells and the statistics of this ICI varies slot-to-slot, the best performing techniques usually choose the transmit powers conservatively so as to minimize the ICI. Otherwise, MCS selection would be significantly affected even for the baseline schemes. So, we conservatively take r_{max} to be between 1 and 2. We also consider $\gamma = 0.1$ for one of the baseline schemes so that a higher number of layers is selected for each UE. Fig. 4 highlights that the proposed scheme provides a significantly higher (> 50%) GM rates compared to the best baseline schemes while requiring a similar level of transmit powers per UE (for most baseline schemes) as shown in Fig. 5. The empirical cumulative distribution functions (CDFs) of the number of spatial layers per UE and the total number of spatial layers per BS are shown in Fig. 6. The trend clearly shows that while the AM rates can be improved by increasing r_{max} at the cost of GM rates, the best balance is achieved for r_{max} between 1.25 and 1.75.

B. Downlink Results

Baseline power allocation: Let $\mathbf{w}_{g,row}^{(k)}$ denote the k^{th} row of \mathbf{W}_g , $k = 1, \dots, n_B$, $g = 1, \dots, n_{RBG}$, where \mathbf{W}_g is the equivalent of $\mathbf{W}_{f,t}$ mentioned in Section II-B at a PRBG level. The columns of \mathbf{W}_g are normalized to unity. Then, the precoder is taken to be $\mathbf{W}_g \leftarrow \sqrt{P} \mathbf{W}_g$ with $P = n_{RBG} P_{ant} / \max_{k=1, \dots, n_B} \left\{ \sum_{g \in \mathcal{G}} n_F \|w_{g,row}^{(k)}\|^2 \right\}$, where $n_F / n_{RBG} = 12$, the number of subcarriers per PRBG.

Baseline PRBG allocation: For lack of a better alternative baseline scheme, we assume that all the PRBGs are allocated to all the UEs. Note that the techniques highlighted in [6], [20] require reinforcement-learning and multiple PRB-looping which are out of scope of this paper.

Baseline UE rank selection: This is done in the same way as for the uplink.

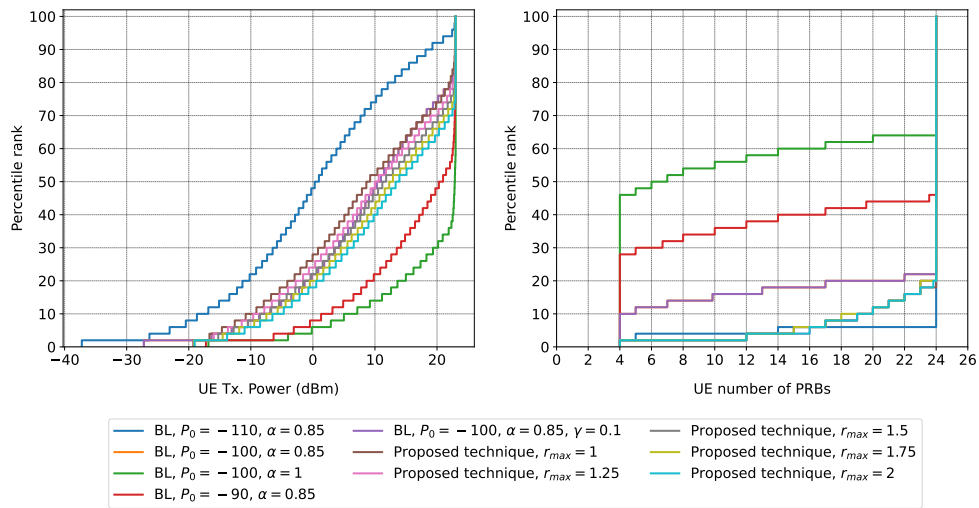


Fig. 5. UL: Percentile ranks of the UE transmit power (left) and the PRB allocation (right) for the case with ICI.

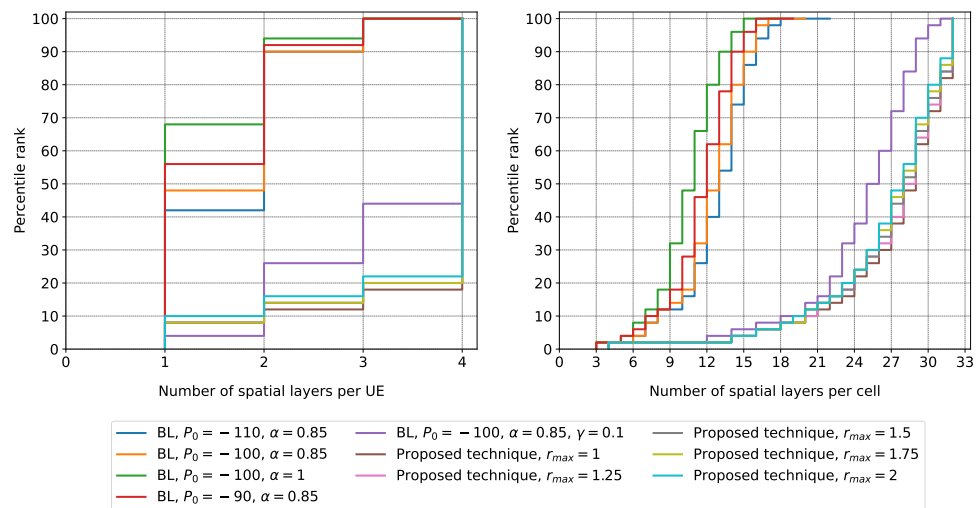


Fig. 6. UL: Percentile ranks of the number of data layers per UE and the number of spatial layers per BS for the case with ICI.

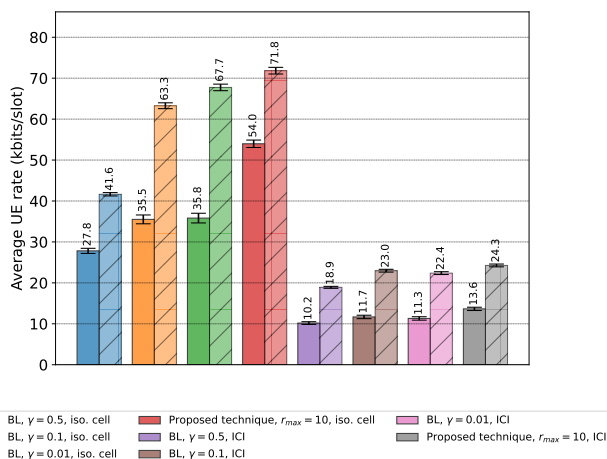


Fig. 7. DL: Plots (with 90% confidence interval) of the UE GM rates (plain bar) and AM rates (hatched bars) in bits/slot.

For the purpose of the estimating the covariance of the interference-plus-noise at the UE (Section III-B), we assume that the UE i measures the interference-plus-noise power σ_i^2 and feeds this scalar back to the serving BS. So, the BS approximates the covariance of this interference-plus-noise as $\sigma_i^2 \mathbf{I}$. Fig. 7 shows the plots of the GM and the AM UE rates for the baseline scheme (with different values of γ for layer selection) and the proposed scheme. The empirical CDFs of the number of spatial layers per UE and the total number of spatial layers per BS are shown in Fig. 8 while the CDFs of the BS transmit power and the PRB allocation are shown in Fig. 9. These plots reveal that for the isolated cell scenario, there is a significant improvement in the GM rates ($> 50\%$ compared to the best baseline scheme) while for the case with ICI, there is around 18% improvement.

VI. CONCLUDING REMARKS

In this work, we proposed a unified framework for jointly performing frequency resource allocation, power allo-

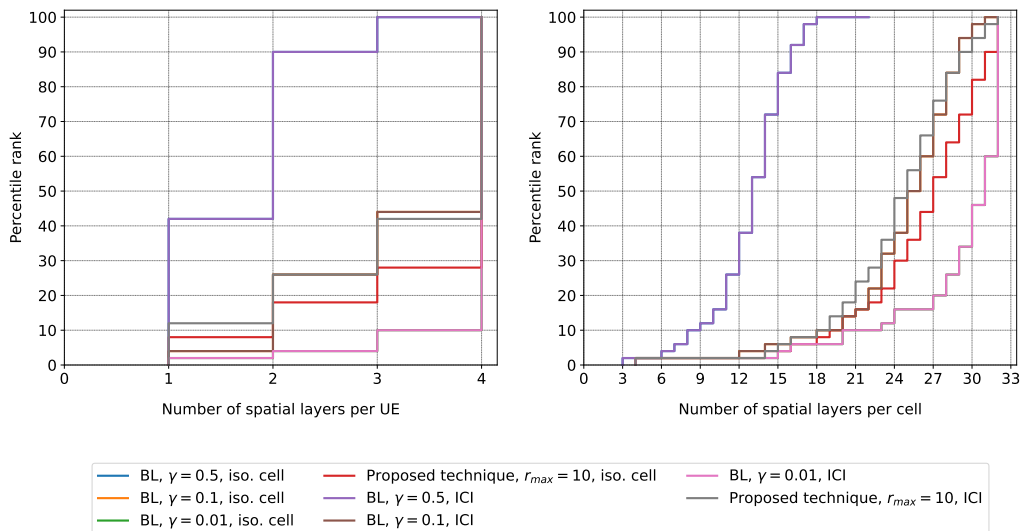


Fig. 8. DL: Percentile ranks of the number of data layers per UE and the number of spatial layers per BS.

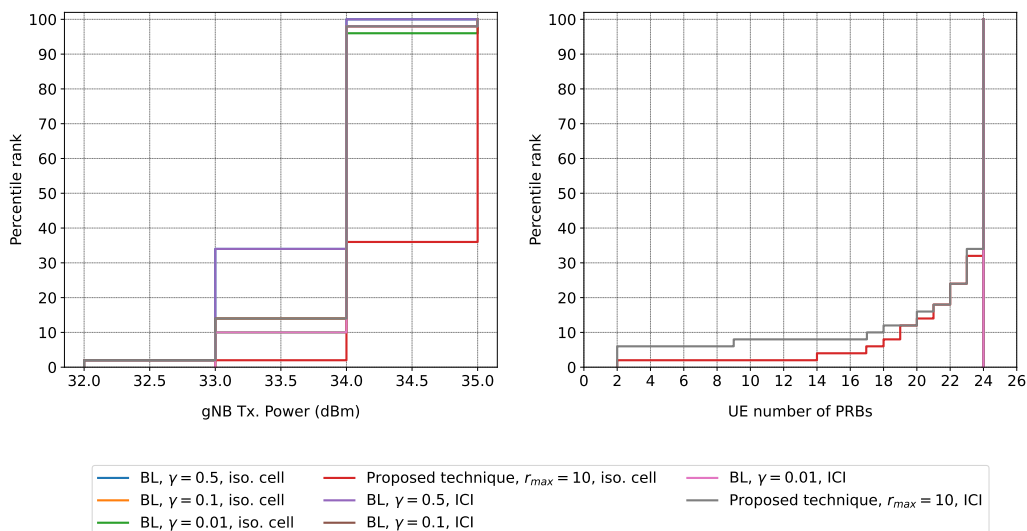


Fig. 9. DL: Percentile ranks of the BS transmit power (left) and the UE PRB allocation (right).

ation/control, and UE rank selection in MU-MIMO systems equipped with linear transceivers. This framework encompasses both uplink and downlink data transmission scenarios. We presented a computationally-efficient algorithm to achieve a near-optimal solution to this problem. Through extensive simulations, we demonstrated that the proposed technique can significantly improve the geometric-mean UE rates compared to existing baseline schemes. While the proposed approach requires the application of interior-point methods in every time slot, we posit the possibility of leveraging supervised or reinforcement learning techniques to guide the solution process. By training these algorithms with expert policies based on the proposed technique, one can potentially eliminate the need for on-the-fly iterative optimization. This avenue presents a promising direction for future research endeavors.

REFERENCES

- [1] V. Stankovic and M. Haardt, "Generalized design of multi-user mimo precoding matrices," *IEEE Transactions on Wireless Communications*, vol. 7, no. 3, pp. 953–961, 2008.
- [2] W.-H. Chou, W.-C. Pao, C.-C. Tsai, T.-Y. Yeh, and J.-Y. Pan, "An adaptive rank selection method in 3gpp 5g nr systems," in *2021 Asia-Pacific Signal and Information Processing Association Annual Summit and Conference (APSIPA ASC)*, 2021, pp. 1912–1916.
- [3] L. Maggi, A. Valcarce, and J. Hoydis, "Bayesian optimization for radio resource management: Open loop power control," *IEEE Journal on Selected Areas in Communications*, vol. 39, no. 7, pp. 1858–1871, 2021.
- [4] X. Sha, J. Sun, T. Wu, and L. Liu, "Adaptive resource allocation based packet scheduling for lte uplink," in *2012 IEEE 11th International Conference on Signal Processing*, vol. 2, 2012, pp. 1473–1476.
- [5] X. Zhao, S. Lu, Q. Shi, and Z.-Q. Luo, "Rethinking wmmse: Can its complexity scale linearly with the number of bs antennas?" *IEEE Transactions on Signal Processing*, vol. 71, pp. 433–446, 2023.
- [6] F. Al-Tam, N. Correia, and J. Rodriguez, "Learn to schedule (leasch): A deep reinforcement learning approach for radio resource scheduling in the 5g mac layer," *IEEE Access*, vol. 8, pp. 108 088–108 101, 2020.
- [7] P. Kela, B. Liu, A. Valcarce *et al.*, "Towards a deep scheduler for allocating radio resources," 2024, in preparation.

- [8] 3GPP, “NR; Physical layer procedures for data,” 3rd Generation Partnership Project (3GPP), Technical Specification (TS) 38.214, 03 2024, version 18.2.0. [Online]. Available: <https://portal.3gpp.org/desktopmodules/Specifications/SpecificationDetails.aspx?specificationId=3216>
- [9] D. Tse and P. Viswanath, *Fundamentals of Wireless Communication*. USA: Cambridge University Press, 2005.
- [10] G. Caire, G. Taricco, and E. Biglieri, “Bit-Interleaved Coded Modulation,” *IEEE Trans. Inf. Theory*, vol. 44, no. 3, pp. 927–946, May 1998.
- [11] M. Uchida and J. Kurose, “An information-theoretic characterization of weighted alpha-proportional fairness,” in *IEEE INFOCOM 2009*, 2009, pp. 1053–1061.
- [12] F. Kelly and A. Maulloo, “Rate control for communication networks: shadow prices, proportional fairness and stability,” *Journal of the Operational Research Society*, vol. 49, pp. 237–252, 1998. [Online]. Available: <https://api.semanticscholar.org/CorpusID:2876114>
- [13] I. I. Dikin, “Iterative solution of problems of linear and quadratic programming,” *Dokl. Akad. Nauk SSSR*, vol. 174, pp. 747–748, 1967.
- [14] A. Wächter and L. T. Biegler, “On the implementation of an interior-point filter line-search algorithm for large-scale nonlinear programming,” *Mathematical Programming*, vol. 106, no. 1, pp. 25–57, Mar 2006. [Online]. Available: <https://doi.org/10.1007/s10107-004-0559-y>
- [15] 3GPP, “NR; Multiplexing and channel coding,” 3rd Generation Partnership Project (3GPP), Technical Specification (TS) 38.212, 12 2020, version 16.4.0. [Online]. Available: <https://portal.3gpp.org/desktopmodules/Specifications/SpecificationDetails.aspx?specificationId=3214>
- [16] S. J. Wright, *Primal-Dual Interior-Point Methods*. Society for Industrial and Applied Mathematics, 1997. [Online]. Available: <https://epubs.siam.org/doi/abs/10.1137/1.9781611971453>
- [17] S. Sun, S. Moon, and J.-K. Fwu, “Practical Link Adaptation Algorithm With Power Density Offsets for 5G Uplink Channels,” *IEEE Wireless Communications Letters*, vol. 9, no. 6, pp. 851–855, 2020.
- [18] K. P. Srinath and J. Hoydis, “Bit-metric decoding rate in multi-user mimo systems: Applications,” *IEEE Transactions on Wireless Communications*, vol. 22, no. 6, pp. 3968–3981, 2023.
- [19] 3GPP, “NR; Physical layer procedures for control,” 3rd Generation Partnership Project (3GPP), Technical Specification (TS) 38.213, 12 2021, version 17.0.0. [Online]. Available: <https://portal.3gpp.org/desktopmodules/Specifications/SpecificationDetails.aspx?specificationId=3215>
- [20] A. Valcarce, P. Kela, S. Mandelli, and H. Viswanathan, “The role of ai in 6g mac,” in *2024 Joint European Conference on Networks and Communications & 6G Summit (EuCNC/6G Summit)*, 2024.